Int J Thermophys (2007) 28:1789–1799
DOI 10.1007/s10765-007-0255-2

# Acoustic Thermometry Results from 271 to 552 K

**D. C. Ripple · G. F. Strouse · M. R. Moldover**

Published online: 8 September 2007


**Abstract** The NIST acoustic thermometer determines the thermodynamic temperature from measurements of ratios of the speed of sound of argon in a nearly spherical cavity. We report recent results for $T - T_{90}$ on 12 isotherms spanning the range 271–552 K. ($T$ is the thermodynamic temperature and $T_{90}$ is the temperature on the International Temperature Scale of 1990.) The results are in excellent agreement with recent acoustic thermometry results reported by Benedetto et al. in the range from 273 to 380 K and with our previously reported results at 303, 430, and 505 K. The combined data sets are sufficiently redundant and sufficiently distributed over the temperature range to support a re-determination of the reference function for standard platinum resistance thermometers for a future temperature scale. The isotherms were analyzed using several methods; the $T - T_{90}$ results and related uncertainties are insensitive to the method chosen. The thermal expansion of the stainless-steel resonator was deduced from the frequencies of the microwave resonances of the cavity. To clearly identify two nearly degenerate eigenmodes in our nearly axially symmetric resonator, two phased coupling probes were used to control the azimuthal angle of the microwave excitation.

**Keywords** Acoustic · Argon · ITS-90 · Primary thermometer · Thermodynamic temperature

## 1 Introduction

Recent acoustic and radiometric measurements of thermodynamic temperature above 273 K have demonstrated that the temperatures $T_{90}$ defined on the International

D. C. Ripple (✉) · G. F. Strouse · M. R. Moldover
Process Measurements Division, National Institute of Standards and Technology, 100 Bureau Drive, Stop 8363, Gaitherburg, MD 20899, USA
e-mail: dean.ripple@nist.gov

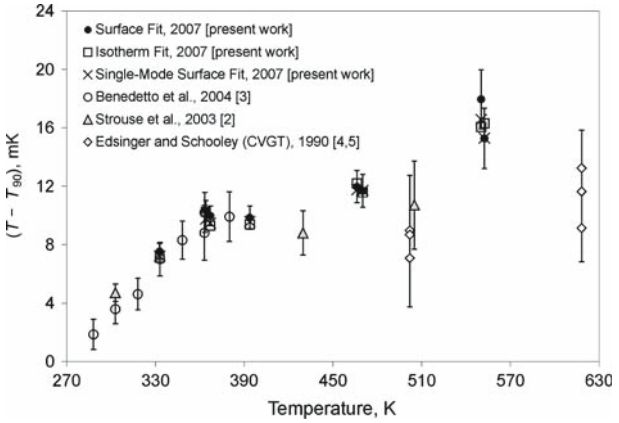


**Fig. 1** Deviation of measured thermodynamic temperature $T$ from $T_{90}$ for recent acoustic determinations and the constant-volume gas thermometry (CVGT) of Edsinger and Schooley [4] and Schooley [5]. For the present work, standard uncertainties are only shown for the recommended Surface Fit

**Table 1** Measured values and standard uncertainties of $(T - T_{90})$ for the Surface Fit. Isotherms near the TPW were obtained in the months 3/2005, 8/2005, 10/2005, and 1/2006

| Month/Year of isotherm | 2/2005 | 8/2005 | 9/2005 | 1/2005 | 9/2005 | 9/2005 | 12/2005 | 12/2005 |
|---|---|---|---|---|---|---|---|---|
| $T$ (K) | 332.856 | 364.101 | 367.170 | 393.808 | 466.231 | 470.213 | 550.746 | 551.863 |
| $T - T_{90}$ (mK) | 7.5 | 10.3 | 10.0 | 9.8 | 12.0 | 11.7 | 17.9 | 15.3 |
| $u_c(k = 1)$ (mK) | 0.6 | 0.7 | 0.7 | 0.8 | 1.1 | 1.1 | 2.0 | 2.1 |

Temperature Scale of 1990 (ITS-90) deviate from true thermodynamic temperature [1–3]. In this article, we describe measurements of thermodynamic temperature with the NIST acoustic thermometer, based on the simple relation between the speed of sound of a monatomic gas and the thermodynamic temperature. By measuring ratios of the acoustic resonance frequencies within a nearly spherical cavity at an unknown temperature $T$ and at a temperature close to the triple point of water (defined as 273.16 K), we obtain the ratio of the argon speed of sound at these two temperatures. With simultaneous measurements of microwave resonance frequencies in the same cavity, we can account for the thermal expansion of the stainless-steel shell enclosing the argon.

As shown in Fig. 1 and Table 1, we have measured the highest thermodynamic temperature yet using high-precision acoustic techniques; we have confirmed the measurements of Benedetto et al. in the range 273–380 K; and we have obtained sufficiently distributed and redundant data in the temperature range 333–552 K to support re-determination of the reference function for standard platinum resistance thermometers (SPRTs). The standard uncertainties achieved are approximately a factor of five lower than the measured deviation of thermodyamic temperature from temperatures on the ITS-90, $T - T_{90}$.

## 2 Basic Theory

We measure thermodynamic temperature, $T$, by exploiting the simple relation between the speed of sound $w$ and $T$:

$$k_{\mathrm{B}}T = (m/\gamma)\, w^2, \tag{1}$$

where, $k_{\mathrm{B}}$ is the Boltzmann constant, $m$ is the molecular mass, and $\gamma$ is the specific heat ratio [4]. In the limit of zero gas density, the ratio of thermodynamic temperature $T$ to the temperature of the triple point of water (TPW), $T_{\mathrm{w}} = 273.16\,\mathrm{K}$, is

$$\frac{T}{T_{\mathrm{w}}} = \left[\frac{w(T)}{w(T_{\mathrm{w}})}\right]^2 = \left[\frac{f_{\mathrm{m}}(T_{\mathrm{w}})}{f_{\mathrm{m}}(T)}\right]^2 \left[\frac{f_{\mathrm{a}}(T)}{f_{\mathrm{a}}(T_{\mathrm{w}})}\right]^2, \tag{2}$$

where, $f_{\mathrm{a}}$ is the frequency of one of the acoustic resonance modes and $f_{\mathrm{m}}$ is the frequency of one of the microwave resonance modes. Corrections are applied to the measured values of both $f_{\mathrm{a}}$ and $f_{\mathrm{m}}$ prior to extrapolation to zero density. References [4–6] give a detailed exposition of the theory, and Ref. [3] gives a concise summary.

In practice, we measure the frequencies of the four lowest non-degenerate, radially-symmetric, acoustic modes [denoted (0,2), (0,3), (0,4), and (0,5)] and the frequencies of the three lowest transverse magnetic microwave triplets (denoted TM11, TM12, and TM13). Each TM triplet is composed of three, nearly-degenerate modes. Therefore, we used a suitably weighted average of the measurements for $f_{\mathrm{m}}$.

## 3 Apparatus

Previous articles [2,7,8] describe the NIST acoustic thermometer. In this section, we give only a brief overview of the apparatus, along with a description of significant changes made to the apparatus since 2003 [2].

The acoustic thermometer consists of a spherical stainless-steel shell, of 3 l internal volume, contained in a stainless-steel pressure vessel and surrounded by three concentric, temperature-controlled aluminum shells. Usually four, and sometimes five, SPRTs were inserted into wells penetrating the pressure vessel and resonator shell to determine the gas temperature on the ITS-90. Argon gas (99.9999 mol% nominal purity), carefully brought to thermal equilibrium with the stainless-steel resonator shell, flowed continuously through the resonant cavity to minimize chemical contamination. A sophisticated pressure control system regulated the gas pressure inside the sphere to effectively eliminate errors from adiabatic heating and cooling. Any impurities in the argon were readily detected using a gas chromatograph mounted directly to the argon gas manifold. Microwave resonance frequencies inside the spherical shell were determined by using a microwave network analyzer connected to 3 mm coupling pins that penetrate the resonator interior. To determine the acoustic resonance frequencies, capacitive electro-acoustic transducers with thin silicon membranes were used as both sound source and detector.

For the present work, we modified the apparatus in an attempt to improve the operation of the thermometer. To reduce spurious acoustic signals caused by mechanical vibrations, which led to inconsistencies in the measured acoustic resonances, we replaced several sections of the cable, previously consisting of platinum wires mounted in hard-fired alumina tubes, with mineral-insulated, metal-sheathed (MIMS) cable. Preamplifier constraints on total cable capacitance precluded the use of MIMS cable for the full length of the triaxial cable connecting the microphone to its preamplifier. The final cable configuration began with a 5 cm long section of MIMS triaxial cable near the microphone. This short section was then welded to a triaxial cable consisting of hard-fired alumina insulators, outer and middle stainless-steel sheaths, and an inner conductor fabricated from 0.5 mm diameter MIMS cable (the conductors inside this MIMS cable were not connected). The new resonator heater was a length of magnesium-oxide insulated thermocouple cable, secured around the equator of the resonator with copper clamps. To reduce outgassing of the MIMS cable to tolerable levels, the sheaths of the triaxial MIMS cable and the heater cable were carefully slit with an abrasive saw every 3 cm for the full cable length.

While the MIMS cable improves the stability of the acoustic signals, we found during the isotherm measurements that our use of MIMS cable in the apparatus was counter-productive. Measurements on the gas chromatograph at 550 K indicated production of large quantities of carbon monoxide and carbon dioxide in the pressure vessel surrounding the resonator. No significant contamination was found in the argon sampled directly from the resonator. Since these gas purity problems have not been observed in previous work with the NIST acoustic thermometer, and since leak-testing revealed no leaks in the pressure vessel or gas manifold, we suspect a chemical reaction involving the hydrogen outgassed from the stainless-steel resonator, magnesium oxide in the MIMS cables, and carbon in the steel components.

No useful signal could be obtained above 552 K. The preamplifier applies a bias voltage of 150 V dc across the capacitor formed by the two plates of the acoustic transducer, through a very high impedance resistor. As the temperature rose and the level of gas impurities increased in the pressure vessel, we noted that transient voltage steps, followed by decays of order 1 s, appeared across the transducer leads, leading to greatly reduced signal-to-noise ratios.

Several minor modifications of the furnace significantly improved the temperature non-uniformities of the resonator. In the previous version, convection from the cable heaters at the bottom of the inner aluminum shell resulted in hot gas collecting near the top of the inner shell, just under the top of the middle aluminum shell. To compensate for this effect, we (a) added vent holes to the top of the middle shell and (b) altered the relative fraction of heat applied to the upper and lower cylindrical portions of the inner aluminum shell.

## 4 Temperature Measurements on the ITS-90

The SPRTs were calibrated as needed at the relevant ITS-90 fixed points before measuring a set of isotherms. Readings of the TPW resistance ($R_W$) were taken before and after thermal cycles of the SPRTs, to monitor possible changes in the SPRTs. Note that

**Table 2** Uncertainty budget for $(T - T_{90})$, with all components given as standard uncertainties in millikelvins

| | $T$ (K) | | | | | | | |
|---|---|---|---|---|---|---|---|---|
| | 333 | 364 | 367 | 394 | 466 | 470 | 550 | 552 |
| *Microwave Frequency Ratios* | | | | | | | | |
| Mode inconsistency | 0.3 | 0.3 | 0.3 | 0.4 | 0.4 | 0.4 | 0.5 | 0.5 |
| Mode sampling | 0.1 | 0.1 | 0.1 | 0.1 | 0.2 | 0.2 | 0.3 | 0.3 |
| Penetration depth | 0.1 | 0.1 | 0.1 | 0.1 | 0.1 | 0.1 | 0.2 | 0.2 |
| Probe and transducer effects | 0.1 | 0.2 | 0.2 | 0.2 | 0.4 | 0.4 | 0.7 | 0.7 |
| *ITS-90 Thermometry* | | | | | | | | |
| $T_{90}$ determination | 0.2 | 0.2 | 0.2 | 0.2 | 0.3 | 0.3 | 0.3 | 0.3 |
| Thermal non-uniformity | 0.3 | 0.3 | 0.3 | 0.3 | 0.4 | 0.4 | 0.3 | 0.3 |
| *Acoustic Frequency Ratios* | | | | | | | | |
| Mode inconsistency | 0.2 | 0.3 | 0.3 | 0.4 | 0.5 | 0.6 | 1.5 | 1.6 |
| Ambiguity in $h$ | 0.1 | 0.2 | 0.2 | 0.3 | 0.4 | 0.4 | 0.6 | 0.6 |
| Pressure | 0.1 | 0.1 | 0.1 | 0.1 | 0.1 | 0.1 | 0.1 | 0.1 |
| Argon thermal conductivity | 0.1 | 0.1 | 0.1 | 0.1 | 0.2 | 0.2 | 0.3 | 0.3 |
| Gas purity | 0.0 | 0.2 | 0.2 | 0.2 | 0.2 | 0.2 | 0.4 | 0.4 |
| *Combined* | | | | | | | | |
| $u_c(k = 1)$ (mK) | 0.6 | 0.7 | 0.7 | 0.8 | 1.1 | 1.1 | 2.0 | 2.1 |

The mode inconsistency for the acoustic frequency ratio was obtained from the Surface Fit

the acoustic isotherm data are taken with decreasing pressure. To best characterize the state of the SPRTs in the zero-pressure limit, we analyzed the data using $R_W$ values taken following completion of each acoustic isotherm above 303 K. The combined uncertainties for the SPRT calibration and $R_W$ stability are listed in Table 2, along with other uncertainty components discussed below. The standard deviation of the mean of the SPRT readings, which accounts for possible thermal non-uniformity of the gas, ranged from 0.3 mK at 273 K to 0.4 mK at 470 K.

## 5 Identification of Microwave Eigenmodes

An auxiliary experiment addressed an important ambiguity in our 2003 work involving the measured thermal expansion of the resonator [2]. Quasi-spherical resonators [9] are intentionally distorted to make all three axes slightly different in length, resulting in a clear splitting of the triplet into three separate peaks. However, the resonator used in the NIST acoustic thermometer predates quasi-spherical resonators and is slightly elongated only along the $z$ axis, resulting in a splitting of the lowest order microwave triplets into an apparent doublet consisting of a singlet with rotational symmetry about the $z$-axis and an unresolved doublet with symmetry in the $x$–$y$ plane. The NIST acoustic thermometer has three separate microwave coupling pins (#1, #2, and #3) penetrating the wall of the spherical shell and connected to a coaxial cable leading to ambient temperature.

In the present work, we did not resolve simultaneous measurements of the $x$ and $y$ eigenmodes, but we could quantitatively determine the superposition of these modes measured for any two of the three microwave transducers. With a ring coupler, we split

the output signal of the network analyzer and introduced a 0° or 180° phase shift on one half of the split signal. The resulting split signals passed through variable attenuators and then on to the microwave coupling pins. The input of the network analyzer was connected to the third coupling pin. By selecting a 0° or 180° phase shift, and by adjusting the attenuators, the two phased coupling probes behaves as a single coupling probe with an adjustable azimuthal angle.

We swept the azimuthal angle over a 180° range, measured the microwave resonances at each angle setting, and fit a model of two resonance functions and a complex background to the measured data. At angles corresponding to excitation of a single eigenmode, the unresolved peak of the doublet consists of a single eigenmode, and the model fits the data to within the statistical precision of the data. At all other angles, the model can only approximately fit the unresolved mixture of two eigenmodes, and the residuals of the fit will increase. If the microwave signal $S$ has an rms noise $\sigma$, and the frequency values are sufficiently close together, we may evaluate $\sigma$ as the root-mean-square (RHS) of the quantity $(S_{i+1} - S_i)/\sqrt{2}$. Here, $S_i$ is the magnitude of the $i$th frequency value of the transmitted microwave signal and $(S_{i+1} - S_i)$ is termed the first difference. Figure 2 compares the RMS of the residuals with $\sigma$. At excitation angles within $\pm 2°$ of 0° and 90°, $\sigma$ and the RMS value of the residuals agree, indicating that at those angles the pure eigenmode is excited. These azimuthal angles of the pure $x$ and $y$ eigenmodes are conveniently close to the 0° and 90° positions of the actual physical coupling probes #1 and #2; connecting the pair #1/#3 to the analyzer gives an excellent approximation to the $z-x$ doublet, and connecting the #2/#3 pair to the analyzer gives the $z-y$ doublet. As a confirmation of this assignment, the apparent half-widths of the $x$ and $y$ modes at these two excitation angles are equal, as one would expect for two modes that differ only by their rotation in the $x-y$ plane. (At intermediate angles, higher or lower apparent half-widths are obtained from the fit.) The phased-excitation experiments were conducted at temperatures of 274 and 625 K. Postulating that the $x$ and $y$ modes will have identical half-widths at excitation angles 90° apart, we found that the eigenmode azimuthal angles were found to shift by less than 2° between the two temperatures, which contributes a standard uncertainty (labeled "Mode sampling" in Table 2) to the thermodynamic temperature of only 0.3 mK at 550 K.

## 6 Microwave Isotherm Measurements

The resonance frequencies of the TM11, TM12, and TM13 microwave triplets were measured in our apparatus concurrently with the acoustic measurements. We applied corrections for the penetration of the microwaves into the resonator shell, the dielectric constant of argon, and the bulk compressibility of the shell. The corrected data for each mode were then extrapolated to zero-pressure. The zero-pressure values of resonance frequency were combined to give a weighted average frequency $\langle f_{\rm m} \rangle = (1/3)\ f_z + (2/3)\ f_{xy}$.

The correction for the penetration depth may be calculated either by using handbook values [10] of the resistivity of 316L stainless steel or by using the measured half-widths $g_{\rm m}$ of the microwave resonances. The deviations $\Delta g_{\rm m}$ of the measured half-widths from the calculated values were in the range $5.5 \times 10^{-6} < \Delta g_{\rm m}/f_{\rm m} <$

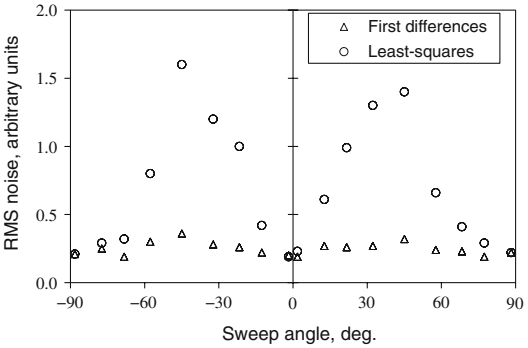


**Fig. 2** RMS noise of microwave spectra at 1.48 GHz at different virtual source excitation angles, as measured by (a) residuals from a least-squares fit and (b) variance of first differences of adjacent frequency points. When the two measures coincide, there are no systematic biases in the residuals

$14 \times 10^{-6}$ and largely independent of temperature, consistent with our 2003 results [2]. We used handbook resistivity values [10] to calculate $g_m$; the small difference in calculated thermodynamic temperature between the two approaches was taken as the standard uncertainty due to imperfect modeling of the penetration depth, as listed in Table 2.

Ratios were formed of the measured resonance frequencies for the TM11, TM12, and TM13 modes, extrapolated to zero-pressure, for an isotherm near the TPW and an isotherm at another temperature. From the standard deviation of these ratios for various isotherm combinations, we obtain the standard uncertainty in thermodynamic temperature resulting from mode inconsistencies, also listed in Table 2.

## 7 Acoustic Measurements

Prior to filling the resonator with argon, the resonator and pressure vessel were evacuated and vacuum baked at 120°C. Then the resonator and pressure vessel were filled with argon of 99.9999 mol% nominal purity. On each isotherm, the resonator was filled with argon at the maximum density of 180 mol·m$^{-3}$. The corresponding pressures ranged from 835 kPa at 505 K to 412 kPa at 273 K. A steady argon flow, from $2.2 \times 10^{-5}$ mol·s$^{-1}$ at 273 K, to $2.9 \times 10^{-4}$ mol·s$^{-1}$ at 550 K, was established to continuously flush impurities (e.g., $H_2$) out of the resonator. The purity of the gas in the resonator was confirmed by measurements with a gas chromatograph at 550 K (see Sect. 3 above) and by runs at 470 K and below where the gas flow was intentionally stopped [8]. All of the tests with gas flow stopped were statistically consistent with no outgassing from the resonator.

At a nominally constant temperature, acoustic data were obtained at 12 decreasing gas densities spanning the range (180–11) mol·m$^{-3}$. At each density, we swept through the resonance of each acoustic mode with both increasing and decreasing frequency, taking measurements at 12 discrete frequency values over a range $\pm 2.8g$ about the central frequency of the (0,2) acoustic mode, and $\pm 2.1g$ about the (0,3), (0,4), and (0,5) modes. (Here $g$ is the resonance half-width.) Both the resonance frequency $f_a$

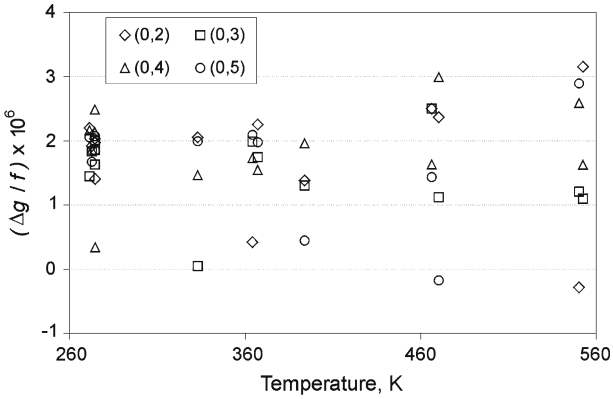


**Fig. 3** Excess acoustic half-widths, in the zero-pressure limit, for the acoustic isotherms

and $g$ are obtained from a fit to the data. The acoustic data were normalized to a single temperature, and corrections were applied to account for: (1) the thermal boundary layer, (2) deviations of the resonator from a perfect sphere, (3) perturbations from the gas ducts, and (4) the compliance of the sphere [6].

The quantity $\Delta g/f$, where the excess half-width $\Delta g$ equals the deviation of observed $g$ value from the $g$ value predicted from the thermophysical properties of argon [11], typically varied from approximately 10 ppm at high gas densities to a zero-pressure limit near 2 ppm. As shown in Fig. 3, the zero-pressure limit of $\Delta g/f$ did not vary with either temperature or mode, and thus cancels in the determination of $T$ [6].

## 8 Analysis and Discussion

To obtain experimental values of the speed of sound, the radius of the cavity $r(T)$ is calculated from $r(T_{\mathrm{W}})$, the known radius at the TPW, and from the microwave frequencies via $r(T) = r(T_{\mathrm{W}})\,\langle f_{\mathrm{m}}(T_{\mathrm{W}})\rangle / \langle f_{\mathrm{m}}(T)\rangle$. The speed of sound is calculated from $r(T)$, and the corrected values of $f_{\mathrm{a}}$ and exact eigenvalues for each mode.

We obtain the zero-pressure limit of the speed of sound by fitting an expansion in pressure to the data [6]:

$$w^2 = A_0\left(1 + \delta_{n,(0,2)}\right) + A_1 p + A_2 p^2 + A_3 p^3 + A_{-1} p^{-1}. \tag{3}$$

The coefficient $A_0$ is proportional to the thermodynamic temperature. The coefficients $A_1$, $A_2$, and $A_3$ are acoustic virial coefficients accounting for the non-ideality of the argon. The small correction $\delta_{n,(0,2)}$ accounts for any systematic deviation of the resonator eigenvalues between mode $n$ and the (0,2) mode, arising from imperfections in our model of the ducts and the absence of corrections for the various joints in the resonator wall. (Such a systematic offset has no effect on the values of $T$ determined from Eqs. (2) and (3), but the residuals of the fit are significantly reduced by including this term.) The coefficient $A_3$ may be estimated from theoretical models of the argon intermolecular potential; by setting $A_3$ to the model value or to zero and examining the

effect on $A_0$, we confirmed that $A_3$ could be neglected in the pressure range studied here.

The coefficient $A_{-1}$ is a measure of the apparent energy accommodation coefficient $h$. Problems with the acoustic signal to noise and parasitic vibrations (microphonics) led to high uncertainties in the $A_{-1}$ coefficient, which in turn limited the reliability of any one determination of the accommodation coefficient. Nonetheless, from our 52 separate determinations of $h$, statistical analysis gives a median value of $1.02 \pm 0.15$, in close agreement with the values near 1 often measured or assumed for machined surfaces. To mitigate the effects of the microphonics on the value of $w$, we assumed $h = 1$ at all temperatures and fit data only for gas densities greater than $20\,\mathrm{mol{\cdot}m^3}$.

The values of $A_0$, $A_1$, and $A_2$ were obtained in three separate ways. In the Isotherm Fit, Eq. (3) was fit to the data of each isotherm independently, with $A_3 = 0$ and $A_{-1}$ fixed by the $h = 1$ assumption. In the Surface Fit, we allowed $A_0$ to vary for each isotherm, but $A_1$ and $A_2$ were taken to be smooth functions of $T$, thereby significantly reducing the number of fitting parameters. We modeled the coefficient $A_1$ as the sum of calculated values obtained from an intermolecular potential of argon [11], plus a

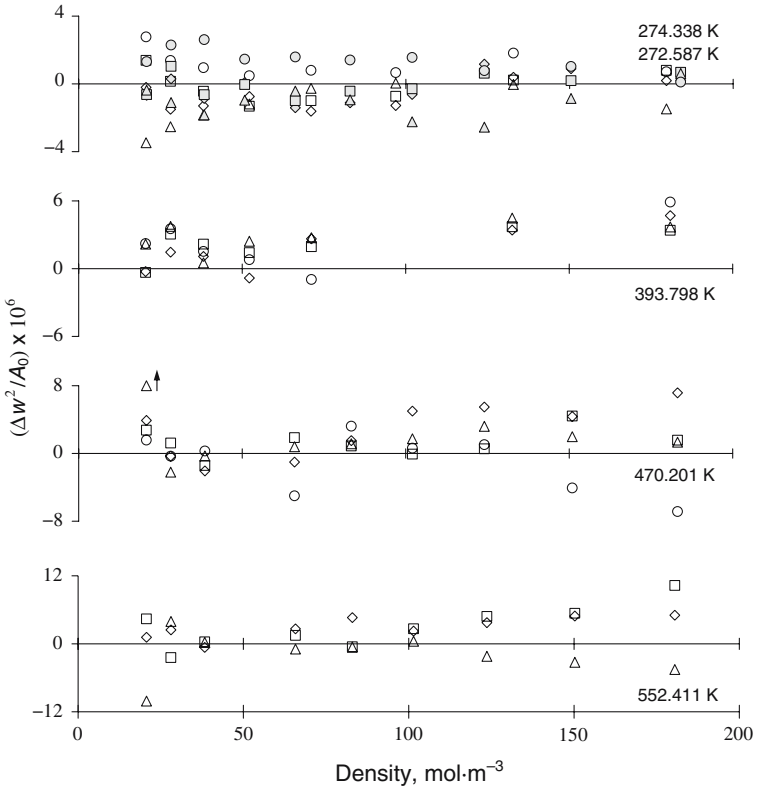


**Fig. 4** Residuals of the surface fit, for several representative isotherms. Data for each acoustic modes are labeled as ◇ for (0,2), □ for (0,3), Δ for (0,4), and ◯ for (0,5). The arrow indicates an outlier for (0,4) discussed in the text

quadratic function in $T$. To model $A_2$, which need not be known to high accuracy, a quadratic function in powers of $1/T$ sufficed. In the Single-Mode Surface Fit, we performed a surface fit to each mode (0,2) through (0,5) independently.

As found in our 2003 work at 505 K, the (0,5) mode at 550 and 552 K apparently coupled to a non-radial shell resonance [2,6] and exhibited anomalous behavior at high densities. Upon removal of this single mode at 550 and 552 K, the reduced chi-square statistic for the Surface Fit dropped greatly from 30 to 14. In all cases, data were weighted according to the observed variance of the data for that particular $p$ and $T$ value. One point on the 470 K isotherm was anomalous as well, but because it carried a low statistical weight, trial removal of this point gave a negligible shift in $T$.

In our 2003 work [2], we selected modes with the most physically plausible values of $h$, and took the standard deviation of the $A_0$ values, as well as the difference between runs with and without $h$ fixed as a measure of mode inconsistency. In the present work, we used all four measured radial modes, and took the uncertainty of $A_0$ as determined in the Surface Fit as the mode inconsistency. An additional uncertainty is added to account for plausible systematic shifts in $h$ by 0.15 over a 250 K span.

Figure 4 shows the residuals for the Surface Fit, which we use to obtain the $T - T_{90}$ values in Table 1. These results, along with $T - T_{90}$ values for the alternate methods of analyzing the data and data from the literature are shown in Fig. 1. For all of our data, the Isotherm and Surface Fit methods give results in excellent agreement [$\Delta$ (Isotherm – Surface) $< u_c(k = 1)$].

In the region of overlap 273–380 K, our measurements are remarkably good in agreement with the work of Benedetto et al. [3]. At higher temperatures, the present results agree with our earlier acoustic measurements within the combined standard uncertainties and with the constant-volume gas thermometry results of Edsinger and Schooley [12] and Schooley [13] to within the expanded ($k = 2$) uncertainties.

**Acknowledgments** We thank John Hurly for supplying us the thermophysical properties of argon, and Wayne Ausherman for his assistance in fabricating the thermometer.

## References

1. J. Hartmann, D.R. Taubert, J. Fischer, in *Proc. TEMPMEKO 2001*, ed. by B. Fellmuth, J. Seidel, G. Scholz (VDE Verlag, Berlin, 2002), pp. 377–382
2. G.F. Strouse, D.R. Defibaugh, M.R. Moldover, D.C. Ripple, in *Temperature: Its Measurement and Control in Science and Industry*, vol. 7, ed. by D.C. Ripple (AIP Conf Proc., Melville, New York, 2003), pp. 31–36
3. G. Benedetto, R.M. Gavioso, R. Spagnolo, P. Marcarino, A. Merlone, Metrologia **41**, 74 (2004)
4. M.R. Moldover, J.P.M. Trusler, T.J. Edwards, J.B. Mehl, R.S. Davis, J. Res. Natl. Bur. Stand. **93**, 85 (1988)
5. M.R. Moldover, J.B. Mehl, M. Greenspan, J. Acoust. Soc. Am. **79**, 253 (1986)
6. M.R. Moldover, S.J. Boyes, C.W. Meyer, A.R.H. Goodwin, J. Res. Natl. Inst. Stand. Technol. (U.S.) **104**, 11 (1999)
7. D.C. Ripple, D.R. Defibaugh, K.A. Gillis, M.R. Moldover, in *Proc. TEMPMEKO '99*, ed. by J.F. Dubbeldam, M.J. de Groot (NMi, Delft, the Netherlands, 1999), pp. 418–423
8. D.C. Ripple, D.R. Defibaugh, M.R. Moldover, G.F. Strouse, in *Temperature: Its Measurement and Control in Science and Industry*, vol. 7, ed. by D.C. Ripple (AIP Conf. Proc., Melville, New York, 2003), pp. 25–30
9. J.B. Mehl, M.R. Moldover, L. Pitre, Metrologia **41**, 295 (2004)

10. J.R. Davis, (ed.), *Stainless Steels* (ASM Int., Materials Park, Ohio, 1994), p. 491
11. S.J. Boyes, Chem. Phys. Lett. **221**, 467 (1994)
12. R.E. Edsinger, J.F. Schooley, Metrologia **26**, 95 (1989)
13. J.F. Schooley, J. Res. Natl. Inst. Stand. Technol. (U.S.) **95**, 255 (1990) and references therein